Electronic Supplementary Information

Mechanical Motion in the Solid State and Molecular Recognition: Reversible Cis-Trans Transformation of an Organic Receptor in a Solid-Liquid Crystalline State Reaction Triggered by Anion Exchange.

Vedichi Madhu, Sabbani Supriya, Ravada Kishore, Indravath K. Naik and Samar K. Das*

1. Synthesis

A. Synthesis of 1,1″-1,4-phenylene-bis(methylene)bis-4,4'- bipyridinium–bromide $[C_{28}H_{24}N_4]Br_2$ (1) and 1,1″-1,4-phenylene-bis(methylene)bis-4,4'- bipyridinium–bis(hexafluorophosphate) $[C_{28}H_{24}N_4](PF_6)_2$

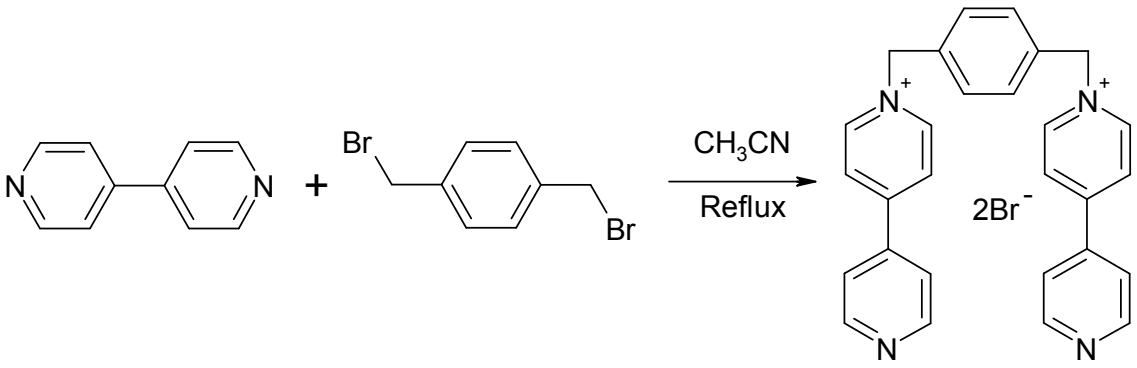

Scheme S1: Schematic representation for preparation of salt $[C_{28}H_{24}N_4]Br_2$ and PF_6 salt $[C_{28}H_{24}N_4](PF_6)_2$ of the cation $[C_{28}H_{24}N_4]^{2+}$ (**1c**).

0.15 g (0.568 mmol) of 1,4-bis(bromomethyl)benzene in 10mL dry acetonitrile was added dropwise to the bromide (**1**) (top) (bottom) receptor

a refluxing solution of 0.5 g (3.2mmol) of 4,4'-bipyridine in acetonitrile (10mL). The resulting reaction mixture was refluxed for additional 2hrs. The bromide salt $[C_{28}H_{24}N_4]Br_2$ (**1**) separated out on cooling to room temperature and the precipitate was filtered, washed with acetonitrile and dried in vaccum. This crude product was dissolved in warm water. The addition of an aqueous solution of NH_4PF_6 results in the isolation of $[C_{28}H_{24}N_4](PF_6)_2$. Yield 0.276 g (~70%).

IR (KBr pellet) (ν/cm^{-1}):3134s, 3074w, 2150w, 1699m, 1639s, 1502m, 1460s, 1421m, 1215s, 1184m, 1010m, 835s, 557s, 515w.

^{1}H NMR (DMSO-d_6): δ 9.28(d, J=6.647, 4H); 8.81(d, J=6.51, 4H); 8.62(d, J=6.48, 4H); 7.97(d, J=6.491, 4H); 7.66(S, 4H); 5.89(S, 4H).

B. Synthesis of [1,1''-1,4-phenylene-bis(methylene)bis-4,4'-bipyridinium][Zn(dmit)$_2$], $[C_{28}H_{24}N_4][Zn(dmit)_2] \cdot 2DMF$ (2)

0.07 g (0.1mmol) of $[C_{28}H_{24}N_4](PF_6)_2$ (see scheme S1) was dissolved in CH_3CN. Subsequently, a CH_3CN solution of $[Bu_4N]_2[Zn(dmit)_2]$ (0.094 g, 0.1mmol) was added to this, whereby a brown color precipitate was formed immediately. The precipitate was filtered, washed with ether and dried in air. Compound $[C_{28}H_{24}N_4][Zn(dmit)_2] \cdot 2DMF$ (**3**) was crystallized from this precipitate in DMF/ ether system (crystallization time duration: 3-4 days at room temperature) as shown in Scheme S2.

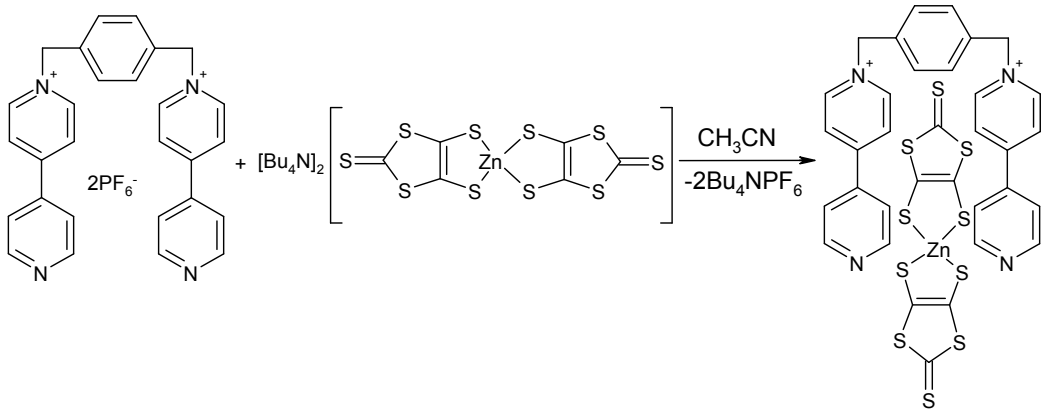

Scheme S2: Schematic representation for the preparation of $[C_{28}H_{24}N_4][Zn(dmit)_2] \cdot 2DMF$ (**2**)

Yield: 0.09 g (90%). IR (KBr pellet) (ν/cm^{-1}) for **2**: 3036m, 1658s, 1635s, 1543m, 1406s, 1215m, 1159m, 1055s, 1028s, 993m, 887m, 790s, 729m, 459s.

^{1}H NMR (DMSO-d_6): δ (ppm) 9.32(d, J=6.847, 4H); 8.85(d, J=4.891, 4H); 8.862(d, J=5.869, 4H); 7.99(d, J=4.891, 4H); 7.66(S, 4H); 5.89(S, 4H).

^{13}C NMR (DMSO-d_6): 31.24, 62.94, 122.42, 126.36, 130.11, 135.80, 141.22, 145.82, 151.46, 153.37, 162.78, 207.31.

C. Synthesis via solid liquid interface reactions: solid to solid transformation without dissolution of the solid

$[C_{28}H_{24}N_4][Zn(dmit)_2]\cdot$ 2DMF (**2**) (solid phase) + $[Bu_4N]Br$ (soln. phase)

$\rightleftharpoons$ $[C_{28}H_{24}N_4]Br_2$ (**1**) (solid phase) + $[Bu_4N]_2[Zn(dmit)_2]$ (soln. phase)

(**equation 1**)

Forward reaction of equation 1 (compound 1 from compound 2)

The compound $[C_{28}H_{24}N_4][Zn(dmit)_2]\cdot$ 2DMF (**2**) (0.370 g, 0.42 mmol) was suspended in saturated MeCN solution (compound **2** is not soluble in MeCN) of $[Bu_4N]Br$ (0.540 g, 1.68 mmol); the crystals of compound **2** loose the color by removing the coordination complex $[Zn(dmit)_2]^{2-}$ into the solution with the formation of pink-colored MeCN solution of $[Bu_4N]_2[Zn(dmit)_2]$ (freely soluble in MeCN) resulting in colorless crystals of compound $[C_{28}H_{24}N_4]Br_2$ (**1**) (0.120 g), which were separated and air dried. The pink-colored MeCN solution of $[Bu_4N]_2[Zn(dmit)_2]$ was stored in an open beaker and evaporated at an ambient condition, whereby the solid crystals of $[Bu_4N]_2[Zn(dmit)_2]$ appeared. This compound was filtered, washed with isopropyl alcohol followed by diethylether. The identity of this solid as $[Bu_4N]_2[Zn(dmit)_2]$ is confirmed by comparing its PXRD pattern with that, simulated from single crystal data of the reported $[Bu_4N]_2[Zn(dmit)_2]$ (Fig. S13, section 3C). It was also characterized by IR spectral studies (Fig. S12, section 3B).

Reverse reaction of equation 1 (compound 2 from compound 1)

The off-white organic salt $[C_{28}H_{24}N_4]Br_2$ (**1**) (0.450 g, 0.6 mmol) and the colored coordination compound $[Bu_4N]_2[Zn(dmit)_2]$ (2.1 g, 2.2 mmol) were added to the MeCN solvent (50 mL) containing dimethylformamide (2.5 mL), and this reaction mixture was stirred at room temperature for seven days ($[C_{28}H_{24}N_4]Br_2$ (**1**) is not soluble in this medium, but $[Bu_4N]_2[Zn(dmit)_2]$ is freely soluble). During this time, the off-white solid becomes colored by anion exchange (colored complex anion $[Zn(dmit)_2]^{2-}$ gets into the crystal from solution phase and Br^- comes out to the solution from the solid phase). After

seven days of stirring, the reaction mixture was filtered and the colored solid was washed with acetonitrile and hexane and the resulting compound $[C_{28}H_{24}N_4][Zn(dmit)_2]\cdot$ 2DMF (**2**) (0.460 g) was dried under air.

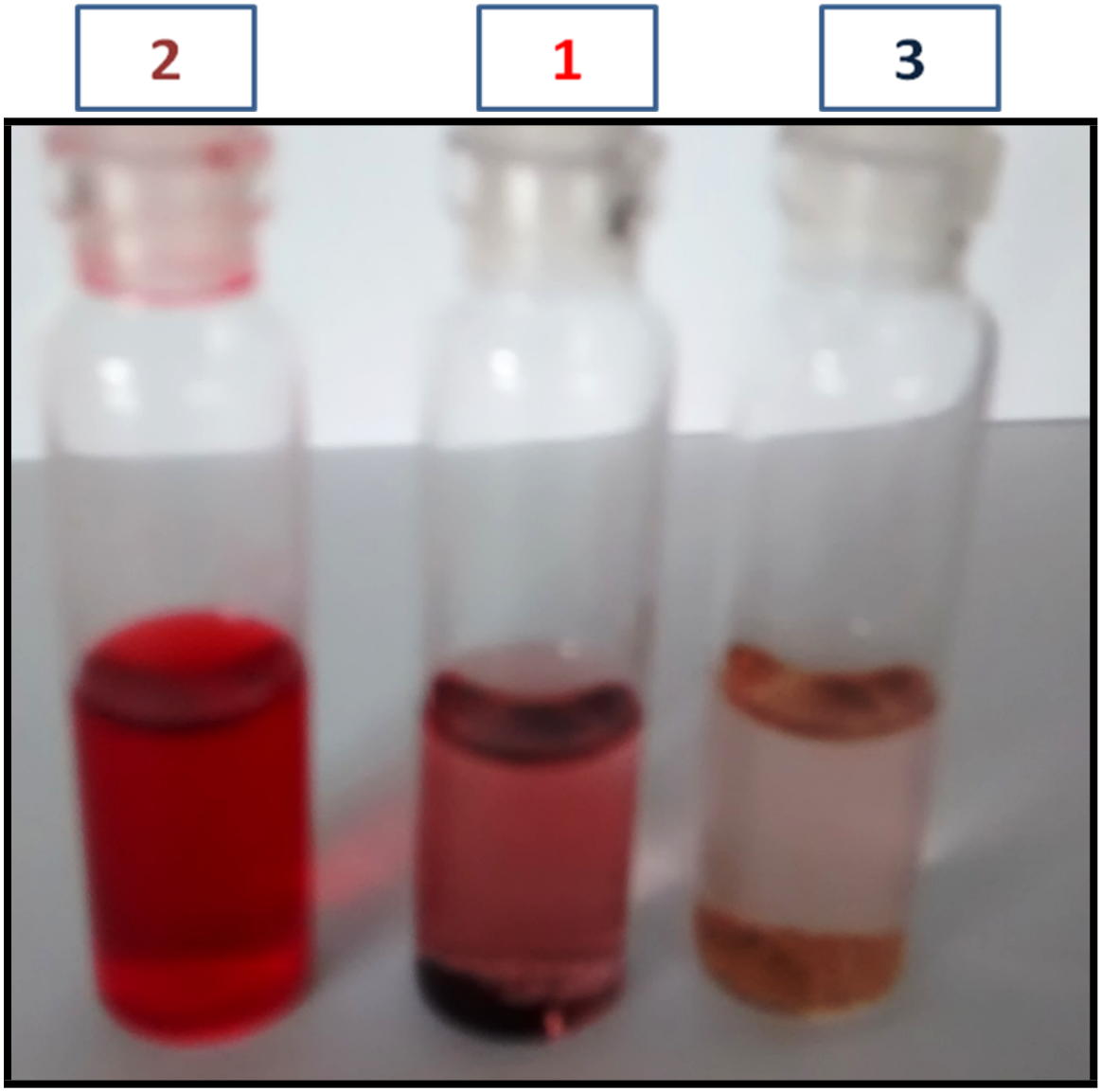

Scheme S3: **1**, $[C_{28}H_{24}N_4][Zn(dmit)_2]\cdot$ 2DMF (**2**) suspended in MeCN dissolving Bu_4NBr; **2**, $[Bu_4N]_2[Zn(dmit)_2]$ solution in MeCN, obtained by stirring **1** at room temperature for 5 minute; **3**, $[C_{28}H_{24}N_4]Br_2$ (**1**) suspended in MeCN, obtained by stirring **1** at room temperature for 5 minute followed by decanting the MeCN solution of $[Bu_4N]_2[Zn(dmit)_2]$ (shown in **2**) and adding MeCN for washing.

2. Crystallography

A. Crystal structure of $[C_{28}H_{24}N_4][Zn(dmit)_2] \cdot 2DMF$ (2)

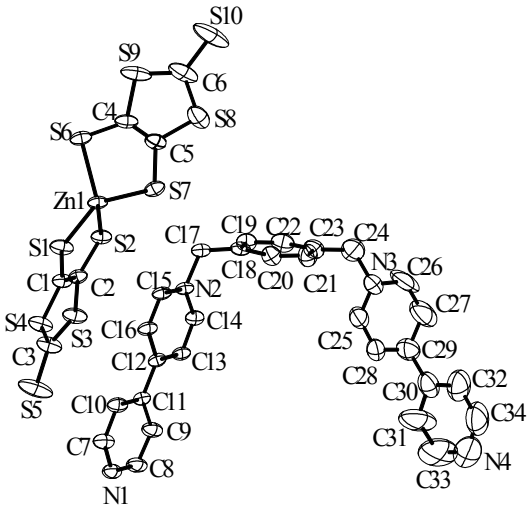

Fig. S1. Thermal ellipsoidal plot of the $[C_{28}H_{24}N_4][Zn(dmit)_2]$ in **2**. Hydrogen atoms and solvent molecules are not shown for clarity.

The usual *trans* conformation of the cation receptor $[C_{28}H_{24}N_4]^{2+}$ (**1c**), found in the crystal structure of compound $[C_{28}H_{24}N_4]Br_2$ (**1**) as shown in Fig. 1 (right) in the main article, is transformed to a cleft-like cis-form (Fig. S2) when it associates with $[Zn(dmit)_2]^{2-}$ anion resulting in the formation of compound $[C_{28}H_{24}N_4][Zn(dmit)_2] \cdot 2DMF$ (**2**). This conformational change occurs through molecular recognition of an inorganic coordination complex anion $[Zn(dmit)_2]^{2-}$ by the cation receptor $[C_{28}H_{24}N_4]^{2+}$ (**1c**). The complex anion, $[Zn(dmit)_2]^{2-}$ exerts π-π stacking interactions to the six-membered aromatic rings of the organic dication as shown in Figs. S2-S4.

π-π Stacking interactions among the organic dications (cation receptors **1c**) are shown in Fig. S4. π-π Stacking interactions among the receptor cations and π-π stacking interactions between cation receptor $[C_{28}H_{24}N_4]^{2+}$ and coordination complex anion $[Zn(dmit)_2]^{2-}$ are together shown in Figs. S3-S4 resulting in the formation of supramolecular zipper (Fig. 2, main article).

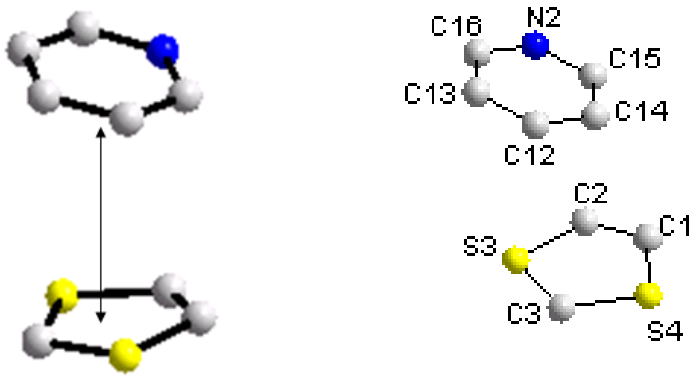

Fig. S2. The origin of π-π interaction between five member ring (C1, C2, C3, S3, S4) of $[Zn(dmit)_2]^{2-}$ and six member ring (C12, C13, C14, C15, C16, N2) of bipyridinium unit. (π-π interactions between cation the $[C_{28}H_{24}N_4]^{2+}$ and anion $[Zn(dmit)_2]^{2-}$: C_t–C_t = 3.928(6)Å, MPS = 3.462Å; C_t–C_t = centroid-centroid distance and MPS = mean plane separation).

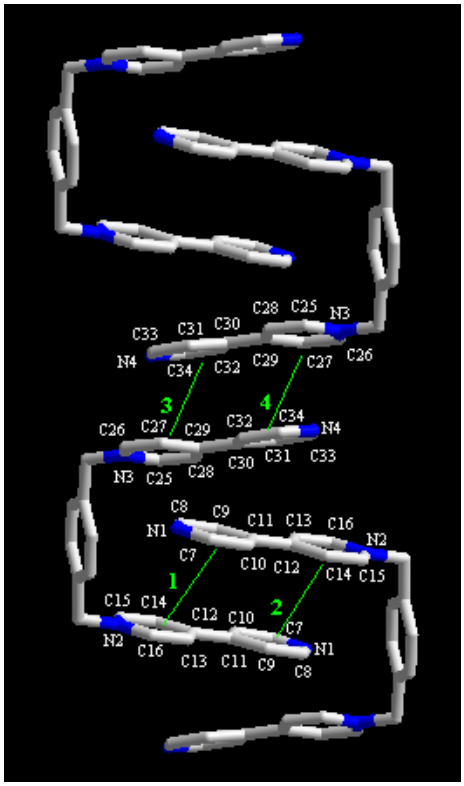

Fig. S3. π-π interactions: 1and 2: C_t–C_t = 3.773(3) Å, MPS = 3.54Å; 3 and 4: C_t–C_t = 3.533(6) Å, MPS = 3.359Å. C_t–C_t = centroid-to-centroid distances; MPS = mean plane separations. Color code: C, gray; N, blue.

1 : π-π interactions between {N2-C15-C14-C12-C13-C16} ring and {N1-C8-C9-C11-C10-C7} ring; 2: π-π interactions between { N1-C8-C9-C11-C10-C7} ring and { N2-C15-C14-C12-C13-C16} ring; 3: π-π interactions between {N3-C25-C28-C29-C27-C26} ring and { N4-C34-C32-C30-C31-C33}ring; 4: π-π interactions between { N4-C34-C32-C30-C31-C33} ring and { N3-C25-C28-C29-C27-C26} ring.

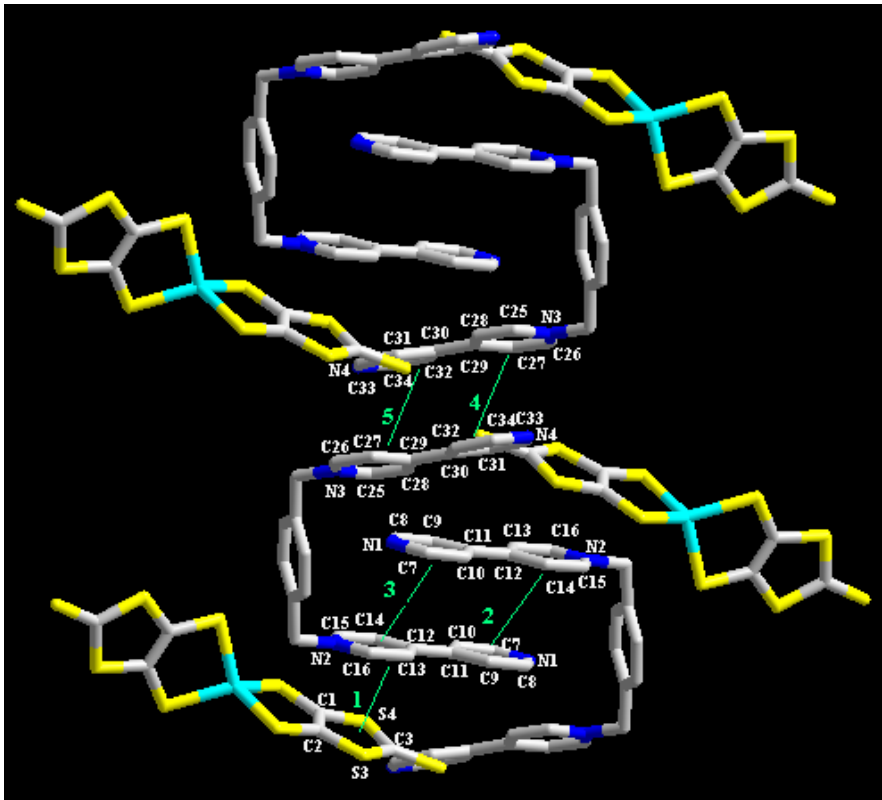

Fig. S4. π-π interactions: 1: C_t–C_t = 3.928(3) Å, MPS = 3.462Å; 3and 2: C_t–C_t = 3.773(3) Å, MPS = 3.54Å; 5 and 4: C_t–C_t = 3.533(6) Å, MPS = 3.359Å. C_t–C_t = centroid-to-centroid distances; MPS = mean plane separations. Color code: C, gray; N, blue; Zn, cyan; S, yellow.

1 : π-π interactions between {C1-C2-S3-C3-S4} ring and {N2-C15-C14-C12-C13-C16} ring; 2: π-π interactions between {N2-C15-C14-C12-C13-C16} ring and {N1-C8-C9-C11-C10-C7} ring; 3: π-π interactions between { N1-C8-C9-C11-C10-C7} ring and { N2-C15-C14-C12-C13-C16} ring; 4: π-π interactions between { N3-C25-C28-C29-C27-C26} ring and { N4-C34-C32-C30-C31-C33}ring; 5: π-π interactions between { N4-C34-C32-C30-C31-C33} ring and { N3-C25-C28-C29-C27-C26} ring.

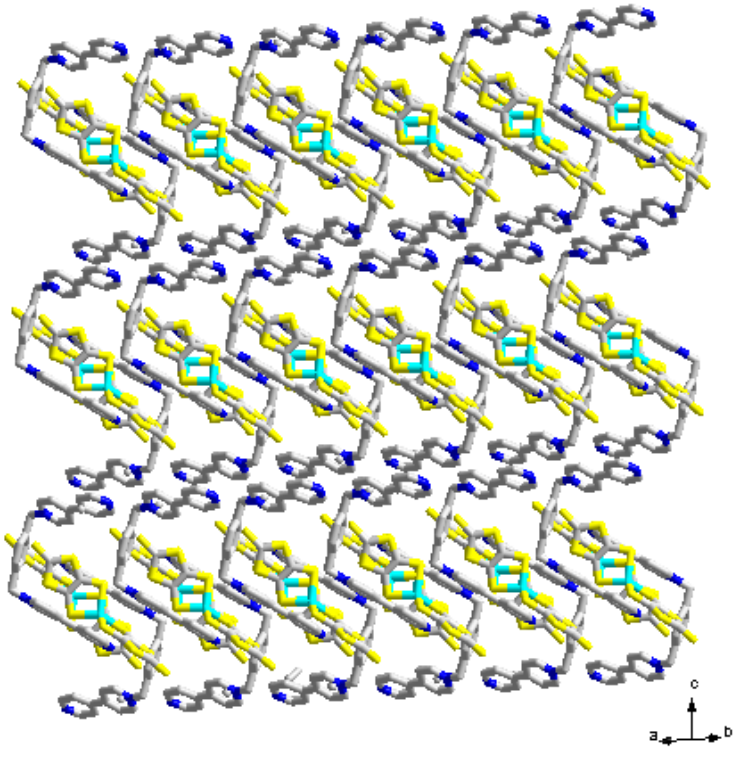

Fig. S5. View (wire-frame representation) of the molecular packing of $[C_{28}H_{24}N_4][Zn(dmit)_2]$ ·2DMF (**2**) (3×3) cells. Color code: Zn, cyan; N, blue; C, gray; S, yellow. The hydrogen atoms and solvent molecules are not shown for clarity.

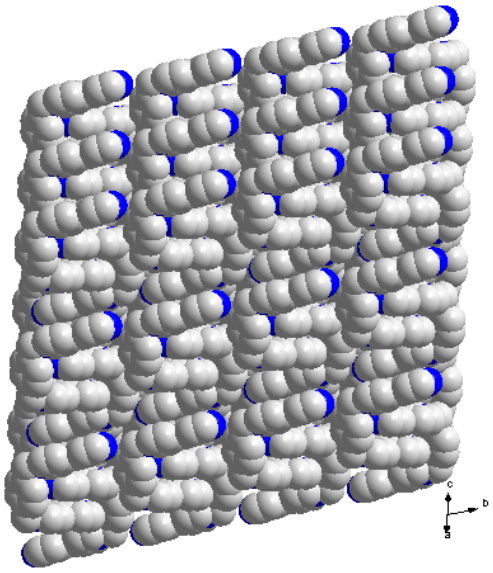

Fig. S6. View (space-filling representation) of the $[C_{28}H_{24}N_4]^{2+}$ cation arrangement in the $[C_{28}H_{24}N_4][Zn(dmit)_2]$ ·2DMF (**2**) (3×3) cells. Color code: N, blue; C, gray.

3. Spectroscopy

A. NMR spectroscopy

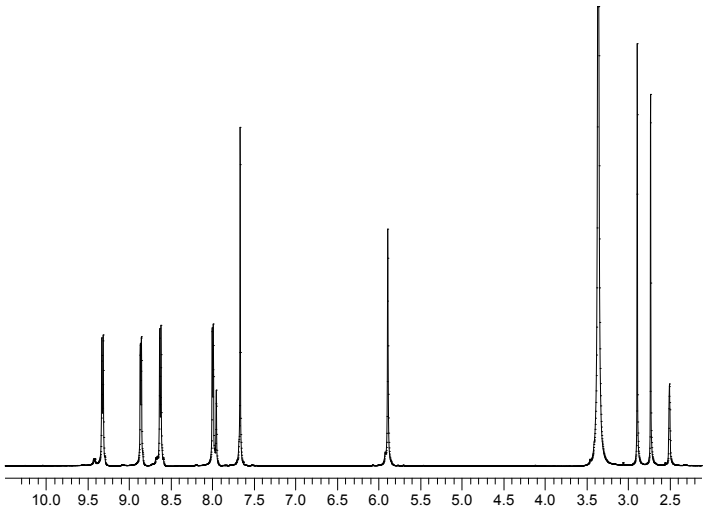

Fig. S7. ^{1}H NMR spectrum of $[C_{28}H_{24}N_4][Zn(dmit)_2] \cdot 2DMF$ (**2**) at 298K.

B. IR spectroscopy

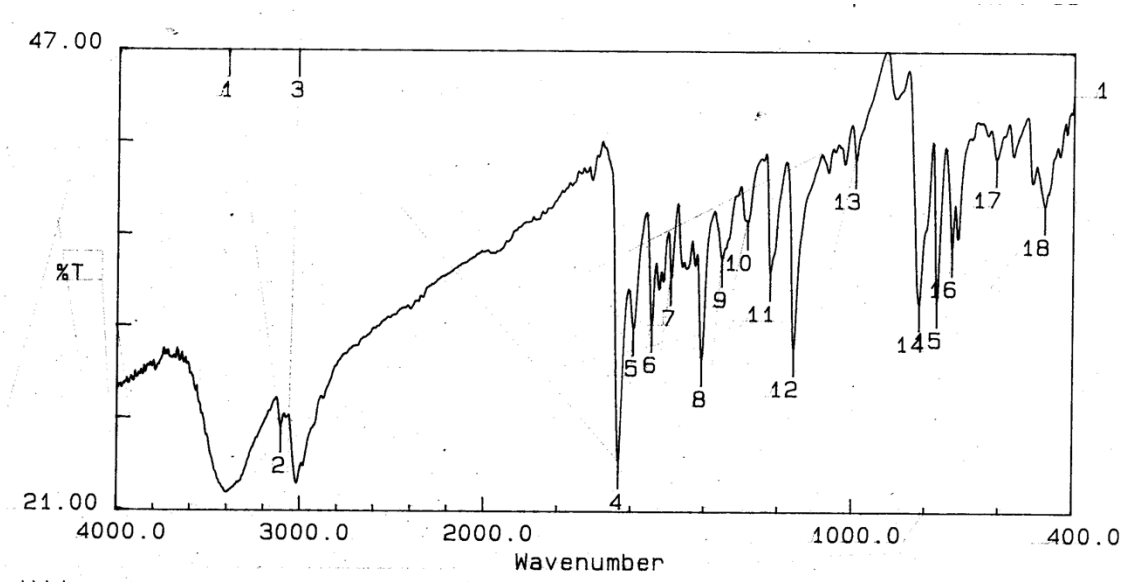

Fig. S8. IR spectrum of $[C_{28}H_{24}N_4]Br_2$ (**1**), obtained from the solid-liquid interlace reaction of $[C_{28}H_{24}N_4][Zn(dmit)_2] \cdot 2DMF$ (**2**) with $[Bu_4N]Br$ dissolved in MeCN solution (solid to solid conversion).

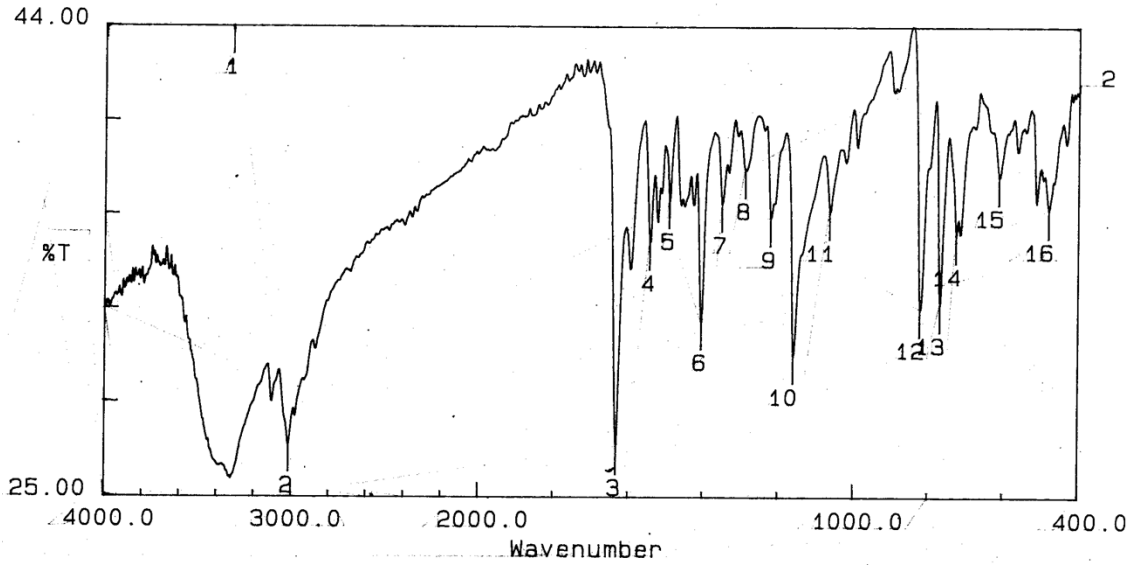

Fig. S9. IR spectrum of parent $[C_{28}H_{24}N_4]Br_2$ (**1**), obtained in a direct synthesis (described in section 1A and scheme S1).

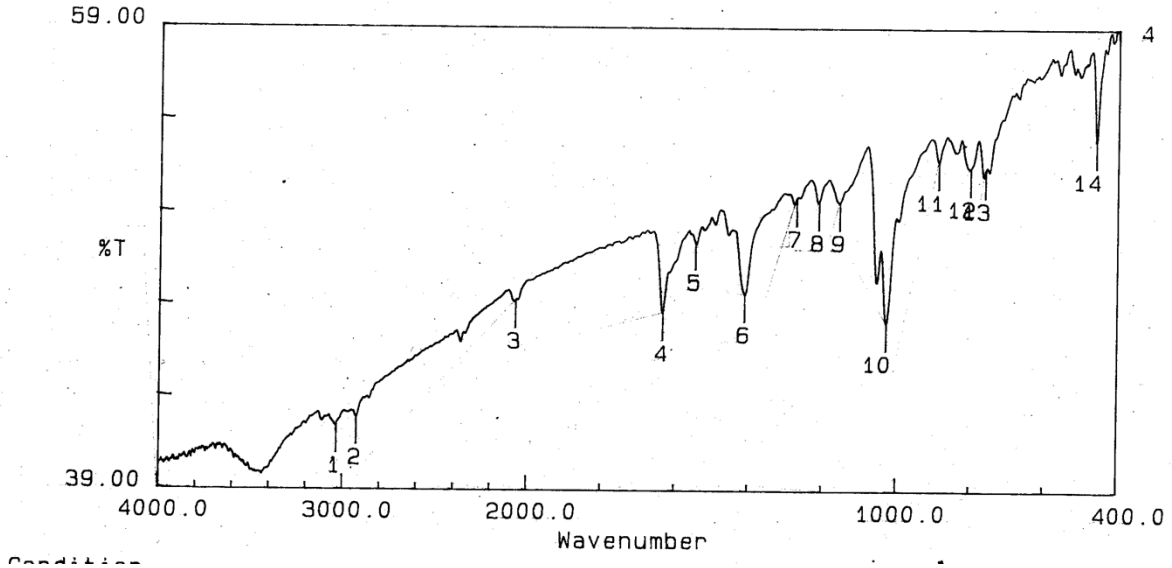

Fig. S10. IR spectrum of the parent $[C_{28}H_{24}N_4][Zn(dmit)_2]\cdot 2DMF$ (**2**) , obtained by the reaction shown in Scheme S2 (Section 1B)

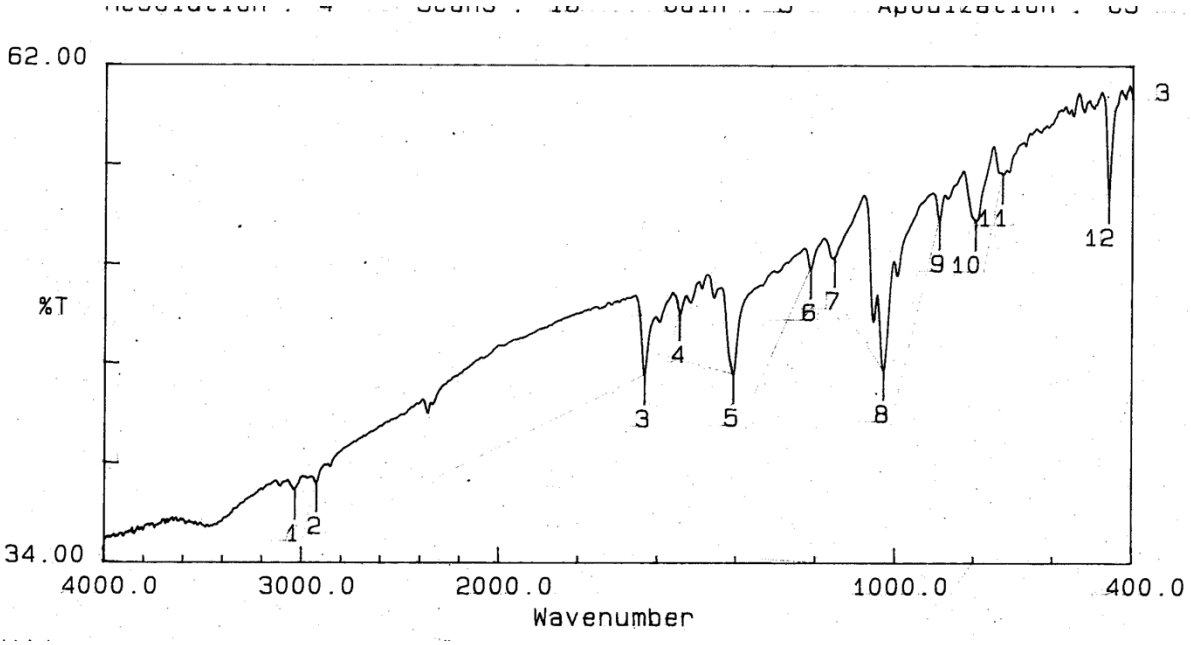

Fig. S11. IR spectrum of the solid $[C_{28}H_{24}N_4][Zn(dmit)_2]\cdot 2DMF$ (**2**) , obtained by the solid-liquid interface reaction shown in reverse reaction of equation 1 (Section 1C)

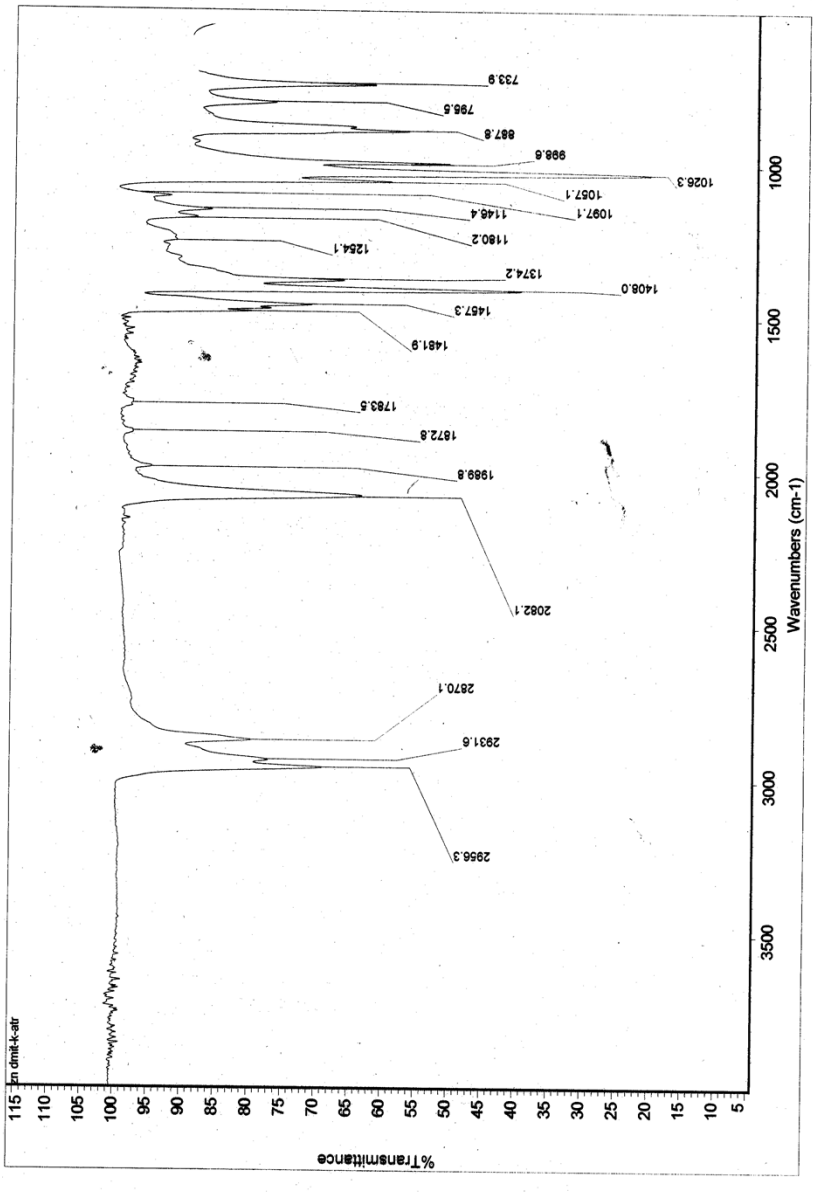
%Transmittance
Wavenumbers (cm-1)
dmik-atr
2956.3
2931.6
2870.1
2082.1
1989.8
1872.8
1783.5
1481.9
1457.3
1408.0
1374.2
1254.1
1180.2
1146.4
1097.1
1057.1
1026.3
988.6
887.8
796.5
733.9

Fig. S12. IR spectrum of the solid $[Bu_4N]_2[Zn(dmit)_2]$, obtained by the solid-liquid interface reaction as shown in the forward reaction of equation 1 (Section 1C)

C. Powder X-ray Diffraction Patterns (PXRDs)

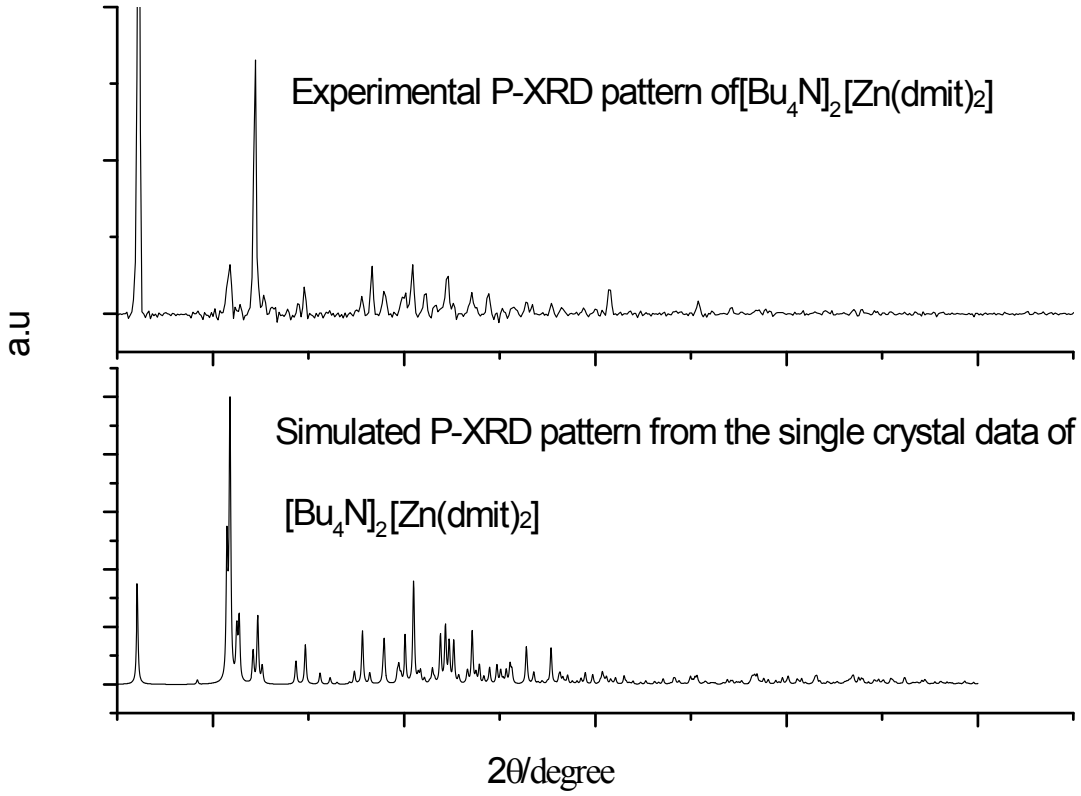

Fig. S13. Powder X-ray diffraction patterns of compound $[Bu_4N]_2[Zn(dmit)_2]$: top, obtained by the solid-liquid interface reaction as shown in the forward reaction of equation 1 (Section 1C); bottom, simulated from single crystal data of $[Bu_4N]_2[Zn(dmit)_2]$ (from reference: Zhao, X.; Wang, Y. L.; Zhang, B. P.; Qin, Y. M.; Yao, J.; Jiang, G. C. *Z. Kristallogr. NCS* **2011**, *226*, 251-253).

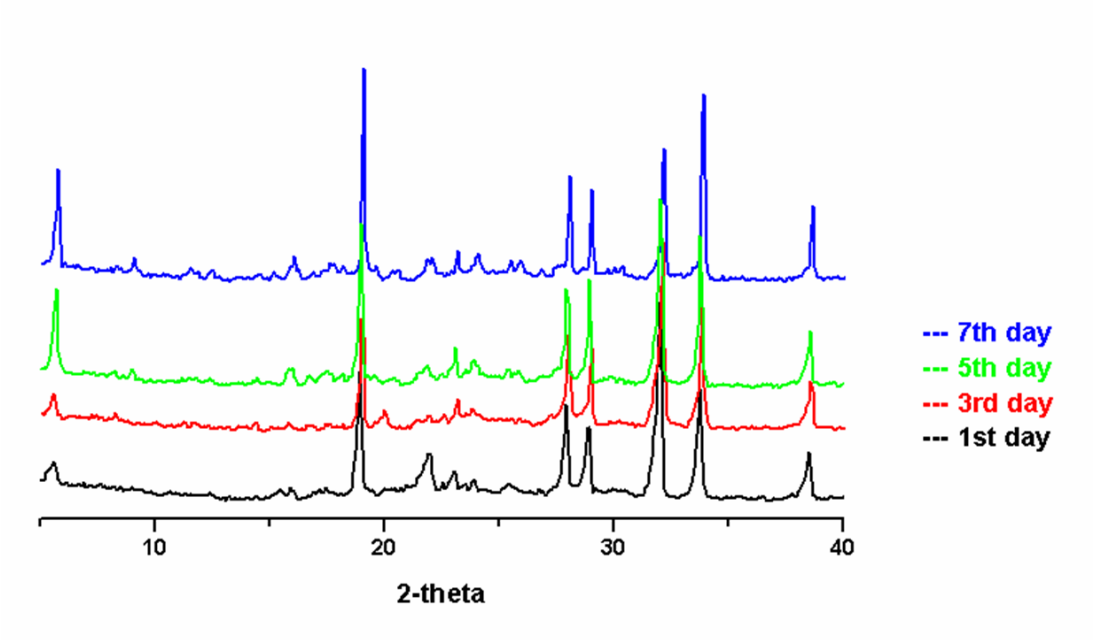

Fig. S14. Powder X-ray diffraction patterns of the intermediate products, obtained by stirring the suspension of $[C_{28}H_{24}N_4]Br_2$ (**1**) (solid phase) in MeCN solution of $[Bu_4N]_2[Zn(dmit)_2]$ (soln. phase). PXRD patterns were taken after one day, after three days, after five days and finally after seven days.

4. Tables

Table S1. Crystal Data and Structural Refinement for Compound $[C_{28}H_{24}N_4][Zn(dmit)_2]$ ·2DMF (**2**)

Compound **2**	
Empirical formula	C34 H24 N4 S10 Zn
Formula weight	874.54
Temperature	100(2) K
Wavelength	0.71073 A
Crystal system, space group	Triclinic, P-1
Unit cell dimensions	a = 11.011(3) A alpha = 71.519(5) deg. b = 11.867(4) A beta = 79.676(5) deg. c = 18.154(6) A gamma = 87.614(5) deg.

Volume	2213.1(12) A^3
Z, Calculated density	2, 1.312 Mg/m^3
Absorption coefficient	1.054 mm^-1
F(000)	892
Crystal size	0.4 x 0.3 x 0.2 mm
Theta range for data collection	1.81 to 24.71 deg.
Limiting indices	-12<=h<=12, -13<=k<=13, -21<=l<=21
Reflections collected / unique	20337 / 7508 [R(int) = 0.0370]
Completeness to theta = 24.71	99.7 %
Absorption correction	None
Refinement method	Full-matrix least-squares on F^2
Data / restraints / parameters	7508 / 93 / 452
Goodness-of-fit on F^2	1.112
Final R indices [I>2sigma(I)]	R1 = 0.0691, wR2 = 0.1876
R indices (all data)	R1 = 0.0847, wR2 = 0.1992
Largest diff. peak and hole	1.722 and -0.798 e.A^-3

Table S2. Bond lengths [Å] and angles [°] for $[C_{28}H_{24}N_4][Zn(dmit)_2]\cdot 2DMF$ (**2**)

C(1)-C(2)	1.353(8)
C(1)-S(1)	1.741(6)
C(1)-S(4)	1.743(6)
C(2)-S(3)	1.742(6)
C(2)-S(2)	1.746(6)
C(3)-S(5)	1.661(7)
C(3)-S(4)	1.711(7)
C(3)-S(3)	1.723(7)
C(4)-C(5)	1.349(10)
C(4)-S(6)	1.737(7)
C(4)-S(9)	1.753(6)
C(5)-S(8)	1.744(7)
C(5)-S(7)	1.753(7)
C(6)-S(10B)	1.691(17)
C(6)-S(10A)	1.693(17)
C(6)-S(8)	1.725(8)
C(6)-S(9)	1.733(8)
C(7)-N(1)	1.325(8)
C(7)-C(10)	1.384(8)
C(8)-N(1)	1.331(8)
C(8)-C(9)	1.378(9)
C(9)-C(11)	1.381(8)
C(10)-C(11)	1.386(8)
C(11)-C(12)	1.493(8)
C(12)-C(13)	1.390(8)
C(12)-C(14)	1.394(8)
C(13)-C(16)	1.364(8)
C(14)-C(15)	1.370(8)
C(15)-N(2)	1.346(7)
C(16)-N(2)	1.343(7)
C(17)-N(2)	1.493(7)
C(17)-C(18)	1.512(9)
C(18)-C(19)	1.374(9)
C(18)-C(20)	1.396(9)
C(19)-C(22)	1.375(10)
C(20)-C(21)	1.370(10)
C(21)-C(23)	1.396(10)
C(22)-C(23)	1.368(10)
C(23)-C(24)	1.509(11)
C(24)-N(3)	1.468(10)
C(25)-C(28)	1.311(11)
C(25)-N(3)	1.319(10)

C(26)-N(3)	1.287(12)
C(26)-C(27)	1.404(16)
C(27)-C(29)	1.424(14)
C(28)-C(29)	1.326(11)
C(29)-C(30)	1.466(12)
C(30)-C(32)	1.326(13)
C(30)-C(31)	1.371(15)
C(31)-C(33)	1.441(18)
C(32)-C(34)	1.402(16)
C(33)-N(4)	1.289(15)
C(34)-N(4)	1.248(14)
S(1)-Zn(1)	2.3239(17)
S(2)-Zn(1)	2.3430(16)
S(6)-Zn(1)	2.3507(17)
S(7)-Zn(1)	2.344(2)
S(10B)-S(10A)	0.705(10)

C(2)-C(1)-S(1)	127.2(5)
C(2)-C(1)-S(4)	114.8(5)
S(1)-C(1)-S(4)	118.0(4)
C(1)-C(2)-S(3)	116.1(5)
C(1)-C(2)-S(2)	127.1(5)
S(3)-C(2)-S(2)	116.8(3)
S(5)-C(3)-S(4)	123.7(4)
S(5)-C(3)-S(3)	124.0(5)
S(4)-C(3)-S(3)	112.3(4)
C(5)-C(4)-S(6)	126.7(5)
C(5)-C(4)-S(9)	115.2(5)
S(6)-C(4)-S(9)	118.2(4)
C(4)-C(5)-S(8)	116.3(5)
C(4)-C(5)-S(7)	126.5(5)
S(8)-C(5)-S(7)	117.2(4)
S(10B)-C(6)-S(10A)	24.1(4)
S(10B)-C(6)-S(8)	135.8(15)
S(10A)-C(6)-S(8)	112.3(14)
S(10B)-C(6)-S(9)	112.0(16)
S(10A)-C(6)-S(9)	135.6(14)
S(8)-C(6)-S(9)	112.0(4)
N(1)-C(7)-C(10)	125.2(6)
N(1)-C(8)-C(9)	124.4(6)
C(8)-C(9)-C(11)	119.8(6)
C(7)-C(10)-C(11)	118.8(5)
C(9)-C(11)-C(10)	116.7(5)
C(9)-C(11)-C(12)	121.9(5)
C(10)-C(11)-C(12)	121.5(5)
C(13)-C(12)-C(14)	117.5(5)

C(13)-C(12)-C(11)	121.0(5)
C(14)-C(12)-C(11)	121.5(5)
C(16)-C(13)-C(12)	120.3(5)
C(15)-C(14)-C(12)	120.1(5)
N(2)-C(15)-C(14)	120.8(5)
N(2)-C(16)-C(13)	121.0(5)
N(2)-C(17)-C(18)	109.1(4)
C(19)-C(18)-C(20)	119.0(6)
C(19)-C(18)-C(17)	121.0(5)
C(20)-C(18)-C(17)	119.8(5)
C(18)-C(19)-C(22)	120.1(6)
C(21)-C(20)-C(18)	120.5(6)
C(20)-C(21)-C(23)	120.1(7)
C(23)-C(22)-C(19)	121.4(7)
C(22)-C(23)-C(21)	118.8(7)
C(22)-C(23)-C(24)	120.7(7)
C(21)-C(23)-C(24)	120.5(7)
N(3)-C(24)-C(23)	110.2(6)
C(28)-C(25)-N(3)	123.4(8)
N(3)-C(26)-C(27)	119.5(12)
C(26)-C(27)-C(29)	119.5(11)
C(25)-C(28)-C(29)	122.2(9)
C(28)-C(29)-C(27)	115.3(9)
C(28)-C(29)-C(30)	124.8(8)
C(27)-C(29)-C(30)	119.8(9)
C(32)-C(30)-C(31)	114.4(11)
C(32)-C(30)-C(29)	124.9(9)
C(31)-C(30)-C(29)	120.7(10)
C(30)-C(31)-C(33)	120.8(13)
C(30)-C(32)-C(34)	120.9(12)
N(4)-C(33)-C(31)	120.9(15)
N(4)-C(34)-C(32)	125.2(13)
C(7)-N(1)-C(8)	115.1(5)
C(16)-N(2)-C(15)	120.2(5)
C(16)-N(2)-C(17)	119.1(5)
C(15)-N(2)-C(17)	120.6(4)
C(26)-N(3)-C(25)	120.0(9)
C(26)-N(3)-C(24)	120.0(9)
C(25)-N(3)-C(24)	120.0(7)
C(34)-N(4)-C(33)	117.8(13)
C(1)-S(1)-Zn(1)	95.1(2)
C(2)-S(2)-Zn(1)	94.61(19)
C(3)-S(3)-C(2)	97.9(3)
C(3)-S(4)-C(1)	98.8(3)
C(4)-S(6)-Zn(1)	94.4(2)
C(5)-S(7)-Zn(1)	93.9(2)

C(6)-S(8)-C(5)	98.2(4)
C(6)-S(9)-C(4)	98.3(4)
S(1)-Zn(1)-S(2)	95.68(6)
S(1)-Zn(1)-S(7)	112.04(7)
S(2)-Zn(1)-S(7)	117.61(6)
S(1)-Zn(1)-S(6)	124.58(6)
S(2)-Zn(1)-S(6)	114.85(6)
S(7)-Zn(1)-S(6)	93.88(6)
S(10A)-S(10B)-C(6)	78(2)
S(10B)-S(10A)-C(6)	78(2)

****